Available online at www.sciencedirect.com
ScienceDirect
Journal of Power Sources 160 (2006) 165–174
JOURNAL OF POWER SOURCES
www.elsevier.com/locate/jpowsour

Short communication

Poly(arylene disulfide)/graphite nanosheets composites as bipolar plates for polymer electrolyte membrane fuel cells

M. Xiao [a], Y. Lu [b], S.J. Wang [a], Y.F. Zhao [a], Y.Z. Meng [a,b,*]

[a] *State Key Laboratory of Optoelectronic Materials and Technologies/Institute of Optoelectronic and Functional Composite Materials, Sun Yat-Sen University, Guangzhou 510275, PR China*
[b] *Graduated School of the Chinese Academy of Science, Beijing 100049, PR China*

Received 6 December 2005; received in revised form 18 January 2006; accepted 25 January 2006
Available online 3 March 2006

Abstract

A poly(arylenedisulfide)/graphite nanosheet (NanoG) composite was first prepared via a direct ring opening polymerization of cyclic (arylene disulfide) oligomers. The graphite nanosheets were prepared by ultrasonic bathing. The dispersion of the NanoG and the morphologies of these composites were investigated by transmission electron microscope (TEM) and scanning electron microscope (SEM). The results revealed the formation of graphite nanosheets in the Poly(arylenedisulfide) matrix. The resulting composites showed good physical properties and superior thermal and electrochemical properties. Compared with a poly(arylenedisulfide)/expanded graphite (EG) nanocomposite, they were better candidates for the bipolar plates of polymer electrolyte membrane fuel cells.

Keywords: PEMFC; Bipolar plate; Graphite nanosheet; Expanded graphite

1. Introduction

Fuel cells are expected to play a major role in the economy of this century and for the foreseeable future [1]. It is anticipated that the development of economic and reliable fuel cells would usher in a sustainable hydrogen age [2]. The polymer electrolyte membrane fuel cell (PEMFC) system is an energy system that can convert hydrogen and oxygen to electricity with water as the only by-product, therefore, this is also environmentally friendly [3].

Polymer electrolyte membrane fuel cells (PEMFCs) are the most promising power sources for road transportation and portable applications. With the bipolar plate accounting for the bulk of the stack, it is desirable to fabricate plates that are as thin and lightweight as possible. Bipolar plates electrically connect successive cells in a fuel cell stack, and also provide the gas supply. Hence, bipolar plate materials have to be inexpensive, easy to machine or shape and lightweight. They must also possess good mechanical properties and thermal stability, with low electrical resistance. Traditionally, PEM fuel cells have been constructed from Poco^{TM} graphite bipolar plates, which have a high bulk electrical conductivity (680 S cm^{-1}) and are resistant to corrosion in the fuel cell environment. Because of the brittleness of graphite, the bipolar plates have to be made several millimeters thick, which makes a fuel cell stack heavy and voluminous; the brittleness of graphite also drives the machining cost of the flow channels on bipolar plates to a prohibitive level—about $10/plate if both the material and machining costs are included. Lately, composite bipolar plates have attracted more interests.

Graphite has been widely used as a conductive filler in fabricating conductive polymer composites. Compared to conventional graphite, expanded graphite (EG) has unique properties. Because it is produced from graphite flakes intercalated with highly concentrated acid, which can be expanded up to a few hundred times their initial volume, the expansion leads to a separation of the graphite sheets into nanoplatelets with very high aspect ratio. These have many unique properties such as excellent electrical and thermal conductivity due to a layered structure [4]. Meanwhile, because of the porous structure, it is possible for monomers and macromolecules to intercalate to produce polymer/EG nanocomposites, which has been reported recently

* Corresponding author. Tel.: +86 20 84114113; fax: +86 20 84114113.
E-mail address: mengyzh@mail.sysu.edu.cn (Y.Z. Meng).

0378-7753/$ – see front matter © 2006 Elsevier B.V. All rights reserved.
doi:10.1016/j.jpowsour.2006.01.085

[5–14] and in previous work in our lab [15], nanocomposites made from cyclo(4,4-oxybis(benzene)-disulfide) (COBDS) and EG were fabricated. Poly(arylene disulfide)s have a high resistance to environmental degradation, a low water vapor transmission, excellent resistance to acids and bases and good adhesion properties [16,17]. These macrocyclic oligomers can directly polymerize when heated to certain temperatures without any initiator and catalyst, therefore the POBDS/EG nanocomposites possess satisfactory properties as bipolar plates. They have good electrical, mechanical and thermal properties, also they could be fabricated through a one step hot molding. However, these nanocomposites have a relatively high porosity and water adsorption, because lots of micropores in EG had not been filled by COBDS and those graphite sheets around cavities tend to overlap each other and form accumulation during processing [19].

In order to solve these problems, we used an ultrasonic treatment to powder EG into graphite nanosheets (NanoG) which was proved to be feasible previously [18]. The aim of this paper is to disperse graphite nanosheets homogeneously, resulting in POBDS/NanoG composites for application as bipolar plates of PEMFC.

2. Experimental

2.1. Materials

Cyclo(4,4-oxybis(benzene)disulfide) (COBDS) ($M_n = 463$ g mol^{-1}, $M_w = 746$ g mol^{-1}, dimer oligomer is the predominant composition) was synthesized according to previous work [17]. The expandable graphite used in this study was supplied by Shandong Pingdu Jiaodong Graphite Company (Qingdao, PR China). The dried expandable graphite was irradiated for a certain time in a microwave oven (WP750, GALANZ), thereby producing expanded graphite (or called graphite worm).

2.2. Samples preparation

The expanded graphite was prepared by making expandable graphite subjected to microwave irradiation for a certain time in a microwave oven (WP750, GALANZ). Compared with the traditional method of heating to a high temperature, it is a cheap and clean [20,21] method. The resulting EG presents a loosely bonded, porous and worm-like rod, consisting of numerous preferentially oriented graphite layers.

Polydisulfide/EG nanocomposites were prepared according to the previous work [15]. The cyclic oligomers were dissolved in chloroform at room temperature. EG was then introduced to the cyclic oligomers solution followed by 5 h stirring. Then, the chloroform was removed using a rotating vaporizer. The resulting COBDS/EG blend powders were dried at 50 °C under vacuum for 24 h, and the dried powders were hot-molded for 30 min at 200 °C under a pressure of 20 MPa.

The polydisulfide/NanoG composites were fabricated by the following method. First, the cyclic oligomers were dissolved in chloroform at room temperature. Then EG was added to the solution gradually during stirring and the solution was sonicated for 8 h until EG was powdered into nanosheets. Subsequently, chloroform was removed using a rotating vaporizer. The resulting blend powders were then dried under vacuum for 24 h at 65 °C, and the dried powders were hot-molded at 200 °C under a pressure of 20 MPa for 30 min. Table 1 lists all the POBDS/NanoG composites fabricated in this work.

2.3. Measurement

A three-point flexure test was performed to measure the flexural properties of these nanocomposites according to ASTM standard D790-96. The moulded nanocomposite plates were cut into $28 \times 3 \times 2$ mm, which were subjected to bending with a support span of 25 mm at a constant cross-head speed of 1 mm min^{-1} using universal testing machine. Five specimens were tested for each set of conditions. The bulk electrical conductivity was measured using SDY-4 four-probe instrument (Guangzhou, PR China). The porosity of each sample was determined according to the ASTM C20 test procedure. Morphologies of the composite bipolar plates were observed on a Hitachi S-520 scan electron microscope (SEM) and JEOL100CX-IImodel transmission electron microscopy (TEM) at 100 kV acceleration voltage. Water adsorption was measured following ASTM D570. The corrosion resistance of the composite bipolar plate was examined with a S1 1287 potentiostat (Solartron company), which included a reference electrode (REF), working electrode (WE), and an auxiliary electrode (AUX). The scanning range was between −0.5 and 0.5 V (versus SCE), and the scanning rate was 10 mV s^{-1}., by using electrochemical measurement techniques. Plots of voltage versus current were recorded. Tafel plots were used to determine the corrosion current. The bipolar plates may not only be corroded in PEMFC environments at open circuit potentials but also may be polarized at the operation potentials of a fuel cell. Thus, those composites were tested under two other conditions as follows: at an operational potential (600 mV_{SCE}) in simulated cathode environment of 0.01 M HCl + 0.01 M Na_2SO_4 bubbled with oxygen, and at an operational potential (−240 mV_{SCE}) in a simulated anode environment of 0.01 M HCl + 0.01 M Na_2SO_4 bubbled with oxygen. SCE represents a saturated calomel reference electrode. The thermal stability of POBDS/NanoG composites from room temperature to 800 °C was determined with a Seiko thermogravimetric analyzer under a protective nitrogen atmosphere. The

Table 1
Compositions of composites made in this work

	Composite A	Composite B	Composite C	Composite D	Composite E
POBDS (wt.%)	80	70	60	50	40
NanoG (wt.%)	20	30	40	50	60

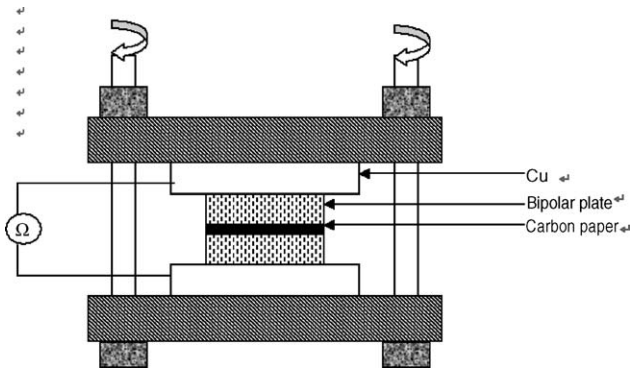

Fig. 1. Schematic illustration of the test assembly for contact resistance.

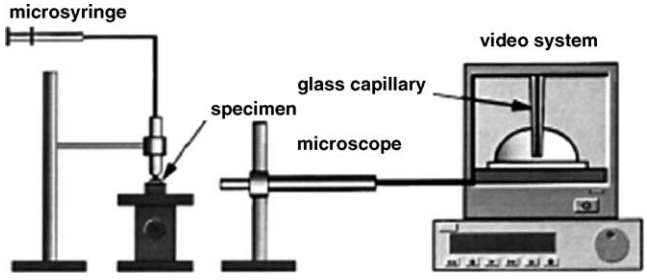

Fig. 2. Apparatus for contact angle measurement.

heating rate used was 20 °C min^{-1}. Contact resistance measurements were conducted using a TOHNICHI DB25N spanner and S1 1287 potentiostat (Solartron company). The assembly torque had a maximum value of 25 N m. A schematic illustration of the experimental set-up is shown in Fig. 1. A carbon paper (Toray TGPH090) was sandwiched between two composite bipolar plates and the assembly was placed between two Copper plates. With the fixed potential between the two electrodes, the electrical current was measured using S1 1287 potentiostat (Solartron company). The assembly torque gradually increased with the use of a TOHNICHI DB25N spanner. The total measured resistance directly obtained according to the relation $R = A \times V/I$ was almost the total contact resistance of a single cell. The water contact angles were measured using the apparatus in Fig. 2.

3. Result and discussion

3.1. Synthesis of aromatic macrocyclic oligomers

It is reported that the synthesis of cyclic aromatic disulfide oligomers could be achieved by using oxidative coupling of dithiols with oxygen catalyzed by copper-salts and an amine as depicted in Scheme 1. Scheme 2 illustrates the melt ring opening polymerization of COBDS. The resulting disulfide polymer could depolymerize in *N*,*N*′-dimethyl acetamide (DMAc) at 100 °C for several hours with a catalytic amount of potassium carbonate and 4,4′-oxybis(benzenethiol). Therefore, COBDS can be recycled, which guarantees a low cost for these composites.

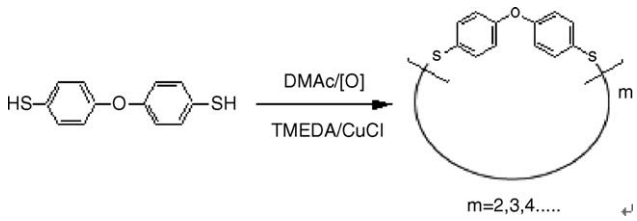

Scheme 1. Catalytic oxidation cyclization of aromatic dithiols.

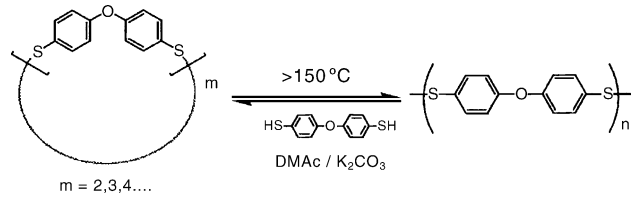

Scheme 2. ROP of cyclic disulfide oligomers and CDP of aromatic polydisulfide.

3.2. Structure of POBDS/graphite nanosheets composites

Conventionally, expanded graphite is prepared in a muffle furnace at temperatures higher than 800 °C. It has been documented that microwave irradiation is widely used in chemical processing. In this work, we fabricated EG via microwave irradiation. The expanded graphite is converted into nanosheets, when it is put into a solution of chloroform and subjected to the ultrasonic irradiation. The as-prepared graphite nanosheets thus possessed a high aspect ratio (width-to-thickness) of around 100–500 [21]. These nanosheets were examined by a TEM technique. It was shown [22] that some of the nanosheets were composed of thinner sheets with a thickness of about 2–5 nm. The galleries in the nanosheets could be penetrated by monomers with aid of sonication. At the same time, sonication was an effective way to disperse the nanosheets uniformly in the solution. The COBDS monomer could more readily penetrate into the nanospace inside the nanosheets with aid of sonication [21]. Thus, upon in situ polymerization, nanodispersion composites could be successfully obtained. SEM images of the cross section of a POBDS/NanoG composite is shown in Fig. 3. The thickness

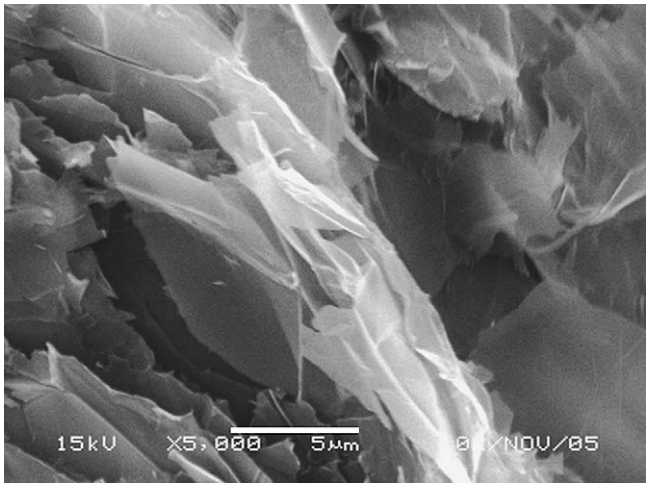

Fig. 3. SEM picture of POBDS/NanoG interior structure.

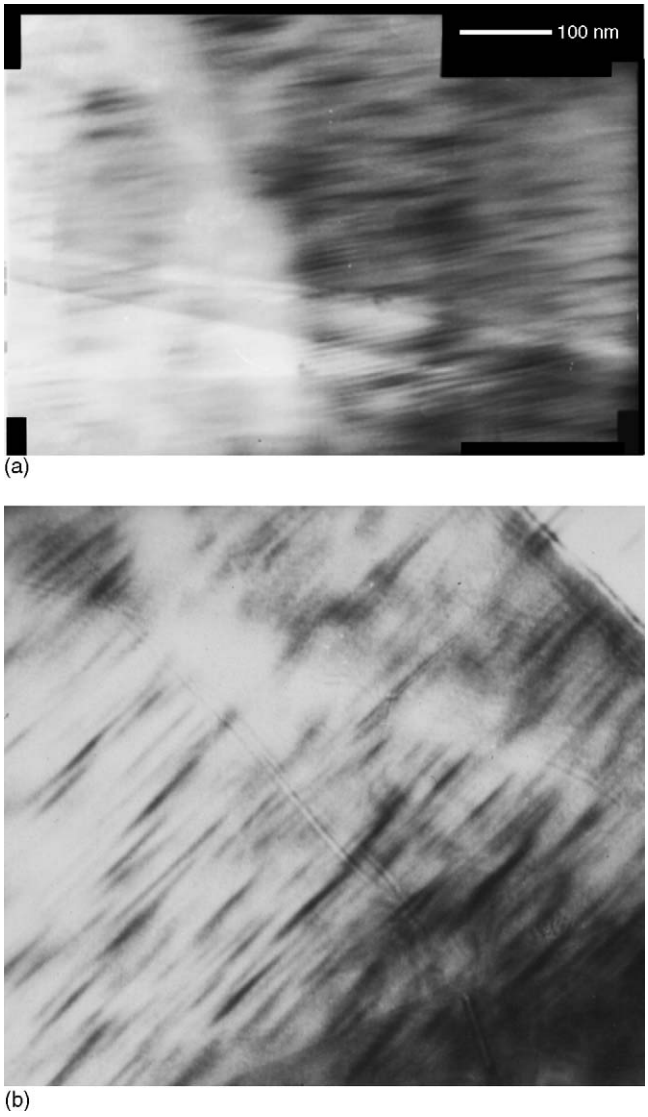

Fig. 4. TEM picture of POBDS/NanoG (a) and POBDS/EG (b).

of the NanoG in the center of the picture like chiffons is on the scale of a nanometer.

The TEM micrographs of the ultra thin section of the POBDS/30%EG nanocomposite and POBDS/30%NanoG composite are illustrated in Fig. 4(a) and (b), respectively. The black solid strips were believed to correspond to graphite nanosheets. It could be seen that the thickness of the graphite nanosheets in both two kinds of composites are nanoscale and the graphite nanosheets had a better dispersion in the POBDS/NanoG composite than that in the POBDS/EG composite. Without the aid of sonication, EG had some graphite layers still unexfoliated (the thicker black solid strips in TEM pictures) and under this condition, absorption of EG was the only driving force for COBDS to penetrate into the micropores and there may be many micropores inside EG that COBDS could not be absorbed into. Therefore, many graphite sheets were accumulated in the processing. Because the graphite sheets had a poor interfacial adhesion, lots of voids formed in the POBDS/EG composites. On the other hand, under ultrasonic irradiation, EG was powdered into nanosheets, which were dispersed well in the solution of chloroform and COBDS. Thus, the homogenous mixture of COBDS and nanosheets was easy to acquire, lowering the occurrence of voids inside POBDS/NanoG composites. Meanwhile, sonication helped COBDS penetrate into the pores of those graphite nanosheets, contributing to a smaller porosity of those composites.

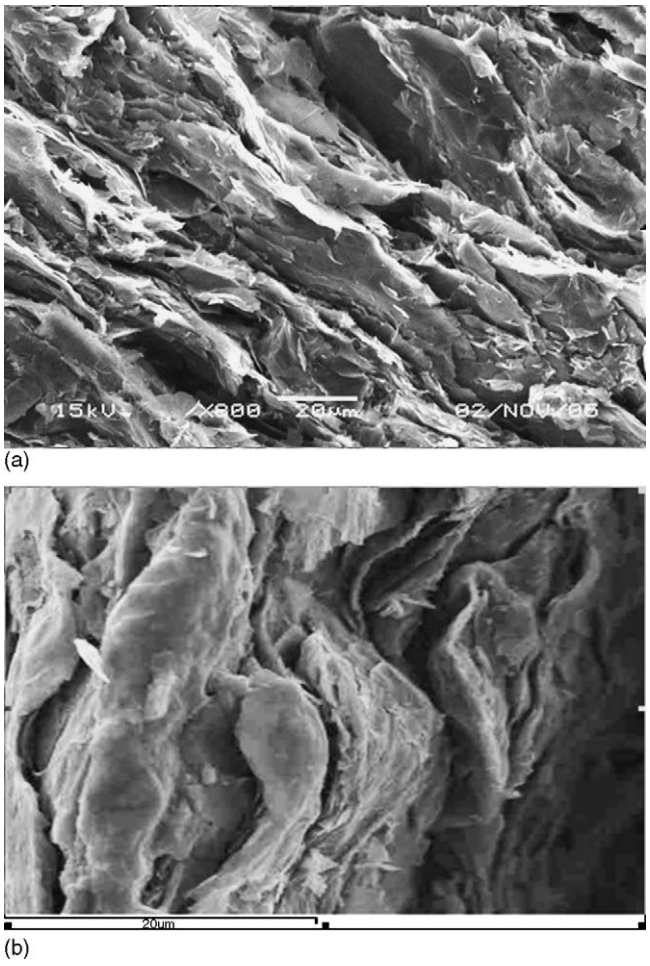

Fig. 5. SEM picture of interior structure of POBDS/NanoG (a) and POBDS/EG (b).

All the above-mentioned observations were verified via SEM images of cross sections and the surfaces of these two kinds of composites, as shown in Figs. 5 and 6. It could be seen that in the composite POBDS/EG, graphite sheets did overlap each other and POBDS was in the form of a big block. However, the graphite nanosheets had better compatibility in the POBDS/NanoG composites and there were fewer graphite sheets accumulating and fewer big blocks of POBDS. Also, Fig. 6 shows that some graphite sheets accumulated in the surface of POBDS/EG composites, however, the surface of POBDS/NanoG composite was more even than that of POBDS/EG, which proved better for the compatibility of the two components in those composites as well.

3.3. Physical properties

Bipolar plates for PEMFCs are supposed to be gas tight, strong, and light, which require them to possess a low porosity,

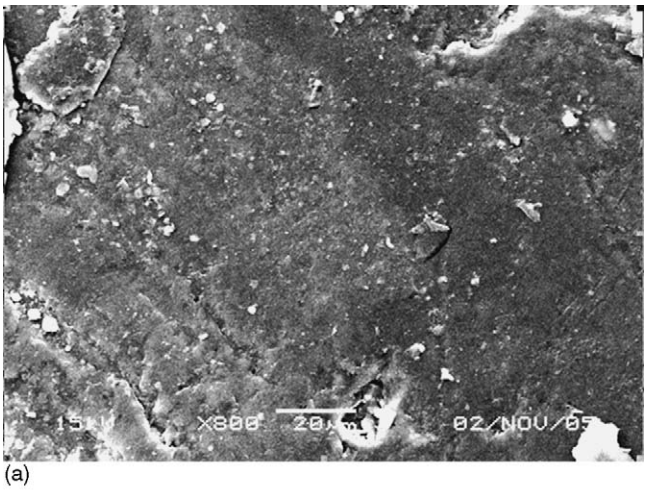

(a)

(b)

Fig. 6. SEM picture of surface of POBDS/NanoG (a) and POBDS/EG (b).

high flexural strength and a low density, respectively. Table 2 presented the physical properties of composites with varying NanoG contents, including the porosity, water adsorption, density and flexural strength. In our previous work, POBDS/EG nanocomposites were fabricated for the application of bipolar plates. However, the high porosity and water adsorption undermined their application as bipolar plates. In this present work, the porosities of the POBDS/NanoG composites were investigated. As shown in Table 2, the porosity of all the POBDS/NanoG composites increased with the content of graphite nanosheets. It was because graphite nanosheets could not be fully wetted by POBDS when their content was higher than a critical value. Thus, lots of graphite nanosheets accumulated and make it more difficult for COBDS to penetrate into galleries between or inside these nanosheets, resulting in a higher porosity. The porosity of POBDS/NanoG increased dramatically from 50% to 60%, demonstrating that the critical value of NanoG wetting was between 50% and 60%. However, the porosity of all those POBDS/NanoG composites was much lower than 0.5%, the target value of bipolar plates of PEMFC.

Table 2
Physical properties of POBDS/NanoG

	Flexural strength (MPa)	Density ($g\,cm^{-3}$)	Porosity (%)	Water adsorption (%)
Graphite	50.00	1.88	1.15	0.58
Composite A	33.72	1.44	0.04	0.03
Composite B	34.88	1.50	0.04	0.03
Composite C	33.11	1.54	0.05	0.03
Composite D	32.05	1.63	0.09	0.05
Composite E	31.24	1.64	0.33	0.20

Bipolar plates account for about 80% of total weight of the PEMFC stack. In order to make PEMFC more portable, it is necessary to lower the weight of bipolar plates. Also, it could be concluded from Table 2 that since the density of POBDS is much lower than that of graphite, the density of the composite bipolar plate increases from 1.44 to 1.64 $g\,cm^{-3}$ with graphite nanosheet content. The density of the plate affects the weight of the fuel cell stack. The maximum density of composite bipolar plate with 60 wt.% NanoG is 1.64 $g\,cm^{-3}$, which is lower than that of a pure-graphite bipolar plate, 1.88 $g\,cm^{-3}$. Therefore, bipolar plates made from POBDS/NanoG composites have a lower weight than pure-graphite bipolar plates.

All the composite bipolar plates in the present work have a low water adsorption, with a minimum of 0.03% and maximum of 0.2%. Because of the porosity increasing with NanoG content, water adsorption increases with its content too. However, the water adsorption of all composite bipolar plates in this work is extremely small.

Flexural strength is another important factor for the bipolar plates of a PEMFC, which should remain unbroken when cell stack was assembled. From the POBDS/NanoG composite series, it is clear that composite E had the lowest flexural strength of 31.24 MPa and composite B had the highest at 34.88 MPa. The reason is that when the NanoG content is lower than 30%, it acts to strengthen the composites. However, at a higher content level, nanosheets tend to accumulate and COBDS would have difficulty in penetrating into all the galleries between or inside the NanoG. Thus, after hot pressing, there must be some nanosheets overlapping each other, resulting in voids in the interior structure, where strain was concentrated when subjected to a certain amount of pressure. Therefore, too much NanoG leads to a low flexural strength.

Compared with POBDS/NanoG composites, POBDS/EG composites had a larger porosity of 5.75%, because of more voids inside, as discussed in Section 3.2. Therefore, POBDS/50%EG composites had a larger water adsorption of 0.75% and a lower density of 1.26 $g\,cm^{-3}$. Fig. 7 presented the flexural strength comparison of the two kinds. They have a similar tendency with filler content. The flexural strength of POBDS/NanoG was a little larger than that of POBDS/EG, demonstrating its better structure.

3.4. Hydrophobicity

It was found that hydrophobicity was one of the important features affecting cell performance particularly at high current densities. In this work, surface hydrophobicity of all the composites was obtained by measuring the water contact angles. The water contact angle of POBDS/20%NanoG, POBDS/30%NanoG, POBDS/40%NanoG, POBDS/50%NanoG,

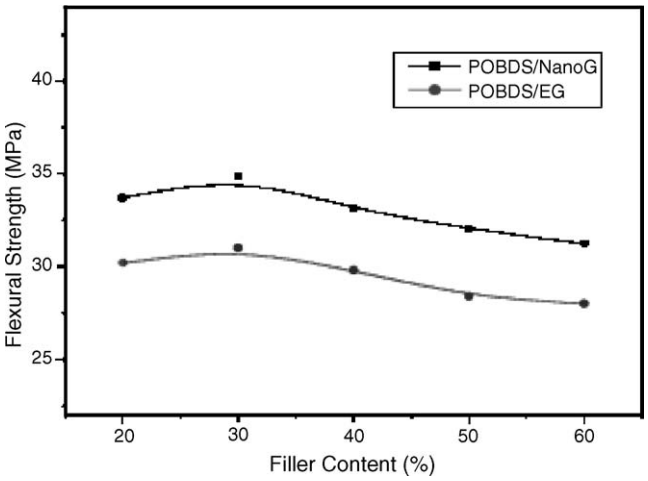

Fig. 7. Flexural strength of POBDS/NanoG and POBDS/EG.

POBDS/60%NanoG composites was 61°, 64.6°, 74.7°, 77.5°, 83.8°, respectively. And the water contact angle of POBDS/50%EG was 72.1°. Fig. 8 presents the pictures of a water droplet on the surface of POBDS/50%NanoG and POBDS/50%EG. Obviously, the surface hydrophobicity gets stronger with increasing NanoG content, due to the strong hydrophobic properties of graphite. And the POBDS/50%NanoG composite was more hydrophobic than the POBDS/50%EG composite. This fact indicates that a water droplet in the gas flow channels of POBDS/NanoG bipolar plates can be swept away more easily by the gas stream under relatively low flow rate conditions. In other words, cells can exhibit higher performance even at low flow rates. This characteristic is important for the improvement of fuel cell system efficiency, because high flow rates result in low oxidant utilization and large power consumption for driving an air compressor or blower to supply air to the fuel cell in the case of using air as an oxidant [23]. In a practical fuel cell stack with a large electrode area, blocking of the gas flow channels by condensed liquid water tends to occur and results in serious degradation as electrode area, reactant utilization and humidifying temperature increases. Therefore, those composites perform better as bipolar plates than POBDS/EG composites. However, they are not as hydrophobic as a graphite bipolar plate whose water contact angle is 93°.

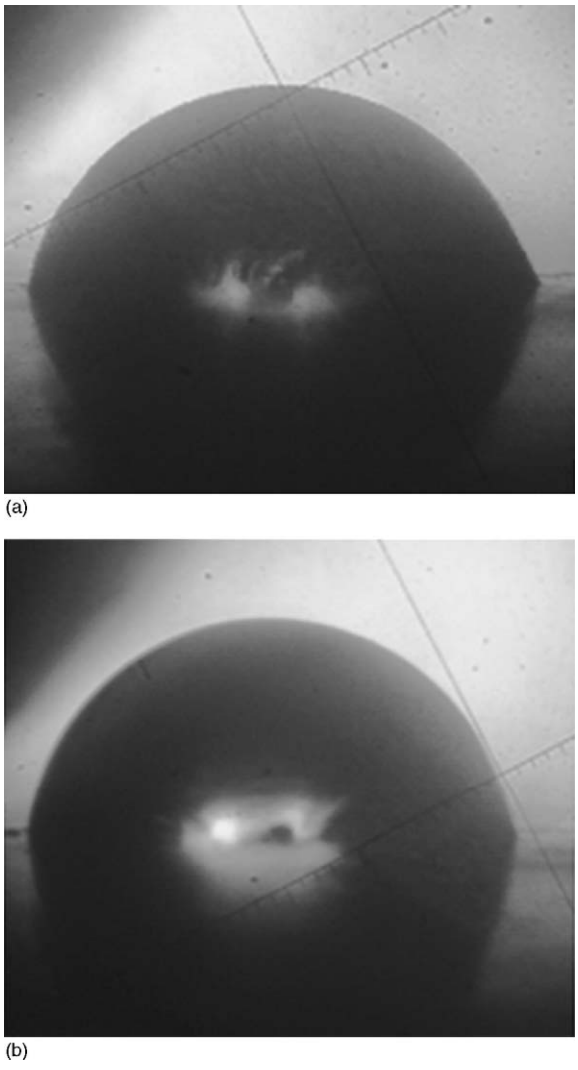

Fig. 8. Picture of a waterdrop on the surface of POBDS/50%EG (a) and POBDS/50%NanoG (b).

3.5. Electrical Properties

3.5.1. Electrical conductivity

Bipolar plates of PEMFC act to electrically connect successive cells in a fuel cell stack and it is well documented that bipolar plates have to possess a electrical conductivity higher than 100 S cm^{-1}. The electrical conductivity of nonporous graphite bipolar plates is 680 S cm^{-1}. Fig. 9 shows the electrical conductivity of composites with different EG or NanoG contents. It could be concluded that the electrical conductivity increased with filler content for the two kinds of composites, due to an increase in the conductive filler-graphite sheets. When the NanoG content was higher than 40%, the electrical conductiv-

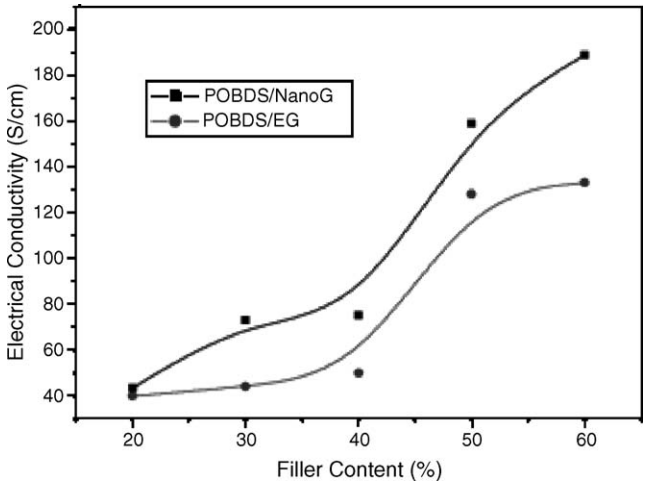

Fig. 9. Electrical conductivity of POBDS/EG and POBDS/NanoG composites.

ity was higher than the target value 100 S cm^{-1}. The electrical conductivity for a composite with 50% and 60% NanoG content was 162 and 188 S cm^{-1}, respectively.

It is clear that POBDS/NanoG composites had a higher electrical conductivity than POBDS/EG with the same conductive filler content. That is because the nanosheets after sonication possessed a higher aspect ratio (width-to-thickness), which is effective to ensure a better conducting network than EG with the same content. Besides, POBDS/20%NanoG and POBDS/20%EG had almost the same electrical conductivity. However, the electrical conductivity of POBDS/30%NanoG composite (72.9 S cm^{-1}) is much higher than that of POBDS/30%EG (44.2 S cm^{-1}). Therefore, it is reasonable to conclude that NanoG is more effective in constructing a conducting network at a relatively low content. Moreover, the electrical conductivity of the two kinds of composites increased dramatically at a content of 40–50%. It is well known that the dramatic increase of electrical conductivity is attributed to the formation of a whole or continuous conducting network in composites. Thus, it is reasonable to argue that NanoG and EG could build up a conducting network in composites at almost the same content.

3.5.2. Contact resistance

A major source of the contact resistance in a fuel cell stack comes from the interface between the gas diffusion layer and the bipolar plate. The contact resistance is governed by the surface topography of the contacting pair. The roughness features of the contacting surfaces decrease the actual area of contact, resulting in a voltage drop across the interface. The pressure applied at the interface brings about an increase in the contact area between fuel cell components, leading to a contact resistance decrease in turn. The interfacial contact resistances between carbon paper and bipolar plates of POBDS/NanoG composites and POBDS/EG composites were investigated, as shown in Figs. 10 and 11. It is shown in Fig. 10 that the contact resistance across the carbon paper and five different POBDS/NanoG bipolar plates decreases with increasing pressure due to the fact

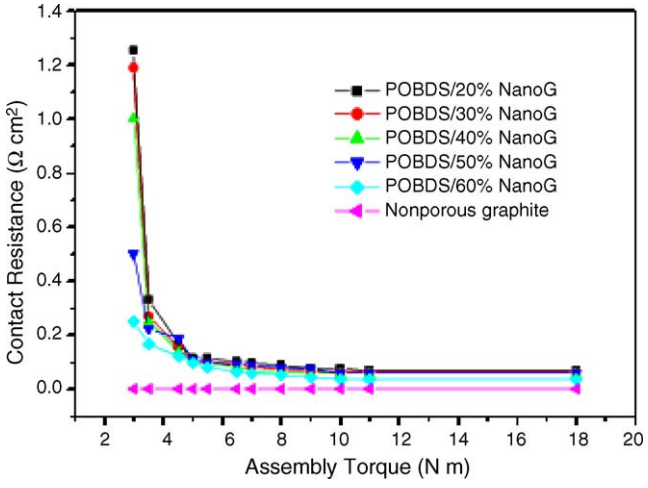

Fig. 10. Contact resistance of POBDS/NanoG composites under different assembly torques.

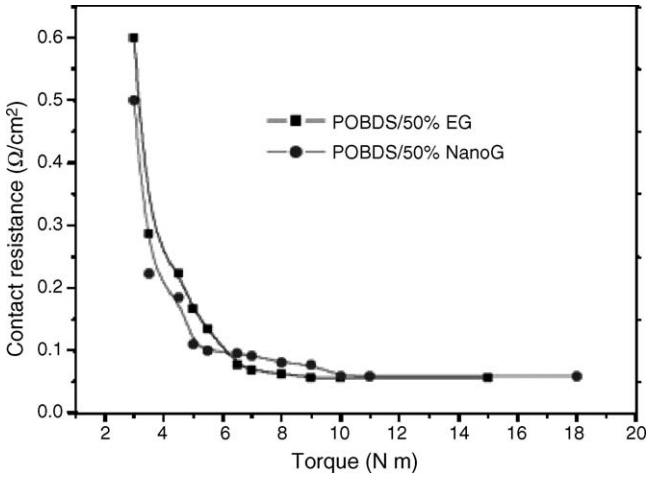

Fig. 11. Contact resistance of POBDS/50%EG and POBDS/50%NanoG.

that the actual area of contact between the asperity structures at the interface increases. Also, it is clear that the contact resistance decreases with the NanoG content, since the graphite has a lower contact resistance with carbon paper than POBDS. And the nonporous graphite bipolar plate has an extremely small contact resistance of about 0.5 mΩ. Fig. 11 compares the contact resistance of POBDS/EG and POBDS/NanoG composite as a function of torque. At low torque, the contact resistance between carbon paper and the POBDS/EG bipolar plate is higher than that between carbon paper and POBDS/NanoG bipolar plate, because the latter has a much smoother surface, as shown in Fig. 5. However, with the increase of assembly torque, the difference becomes smaller. And they are almost the same after 10 N m.

3.5.3. Polarization curves

A Solartron 1287 potentiostat was used for the corrosion test which included a reference electrode (REF), working electrode (WE), and an auxiliary electrode (AUX). The scanning range was between −0.5 and 0.5 V (versus SCE), and the scanning rate was 10 mV s^{-1}. The corrosion behavior of composites was investigated in a simulated proton exchange membrane fuel cell environment i.e. 0.01 M HCl + 0.01 M Na_2SO_4 bubbled with oxygen, using electrochemical measurement techniques. Typical Tafel plots of the different POBDS/NanoG composites after 1 h immersion are shown in Fig. 12. The Tafel slopes are all very similar. The corrosion currents were obtained from the Tafel region of the polarization plot. Table 3 gives values of the corrosion current densities for those composites. These data lead to the conclusion, which can be deduced from Table 3, that more NanoG leads to a decreased corrosion current density, due to the excellent corrosion resistance of graphite. The corrosion current density of all composites is lower than 10^{-6} A cm^{-2}, which demonstrates excellent corrosion resistance of those composites.

Fig. 13 shows the polarization curves of the POBDS/60%NanoG composite and the POBDS/60%EG composite. The two composites have a very close corrosion potential and Tafel slope. The corrosion current density of POBDS/60%NanoG composite and POBDS/60%EG composite is 4.2×10^{-8} and

Table 3
Corrosion current densities with different NanoG content

	Composite A	Composite B	Composite C	Composite E	Graphite
i_{corr} ($\mu A\,cm^{-2}$)	0.39	0.11	0.1	0.04	0.04

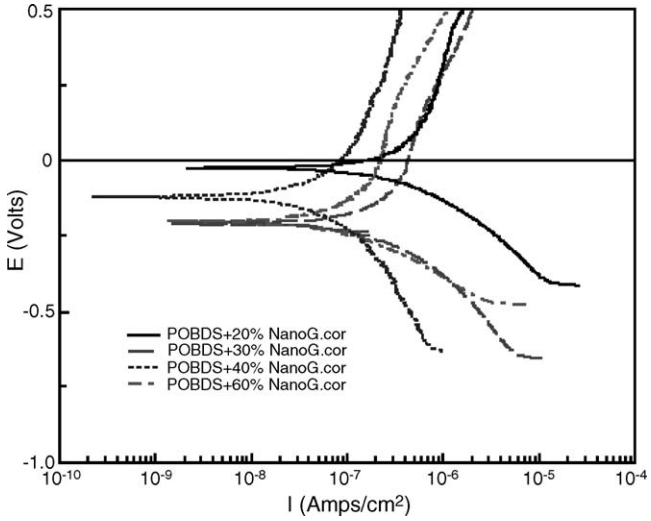

Fig. 12. Polarization curves of POBDS/NanoG composites.

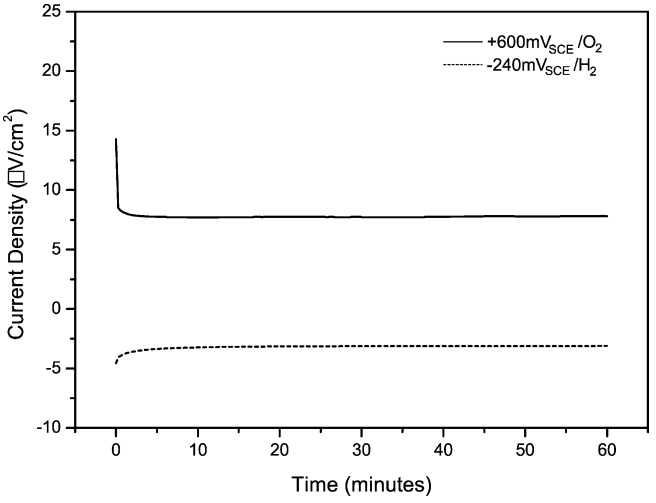

Fig. 14. Fig. 2 Plots of i vs. time for POBDS/50%NanoG potentiostatically polarized in solutions (80 °C) at 600 mV_{SCE} under O_2 condition and at −240 mV_{SCE} under H_2 condition, respectively.

1.7×10^{-6}, respectively. It is obvious that POBDS/NanoG composite has a better corrosion resistance than the POBDS/EG composite. The reason is probably that POBDS/NanoG had better structure and surface properties. The surface roughness creates minute potential differences between the peaks and the valleys in the electrochemical environment. The peaks have a stronger electric potential which leads to a more rapid corrosion. The pictures by SEM of the surface morphology are shown in Fig. 5. The surface of POBDS/NanoG is smoother than that of POBDS/EG, which is helpful in the improvement of corrosion resistance.

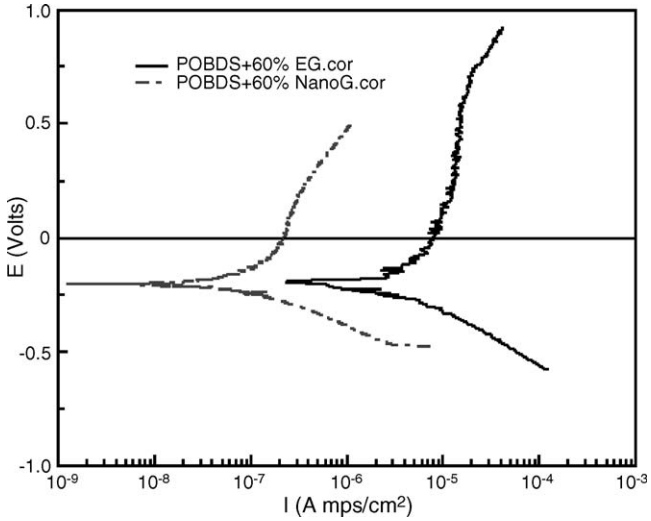

Fig. 13. Polarization curves of POBDS/50%EG and POBDS/50%NanoG.

3.5.4. *Current transients at the operational potentials of the fuel cell*

After the above measurements of polarization curves for all these composites, the current transients were determined and are shown in Fig. 14. The polarization current of the POBDS/50%NanoG specimen at 600 mV_{SCE} in O_2 bubbled solution fluctuated near 7.7 $\mu A\,cm^{-2}$, while the polarization current at 240 mV_{SCE} in H_2 bubbled solution oscillated around $-3.1\ \mu A\,cm^{-2}$. No degradation was observed after the potentiostatic measurements about 1 h. The current transients of other composites are listed in Table 4.

3.6. *Thermal stability*

Thermal stabilities of those composites were determined by thermal gravimetric analysis. Fig. 15 shows TGA curves of POBDS/NanoG composites at different NanoG contents.

Table 4
Current transients of POBDS/NanoG composites

	Current density[a] ($\mu A\,cm^{-2}$)	Current density[b] ($\mu A\,cm^{-2}$)
Graphite	0.32	−0.13
POBDS/20%NanoG	8.8	−4.5
POBDS/30%NanoG	8.3	−4
POBDS/40%NanoG	8.1	−3.6
POBDS/50%NanoG	7.7	−3.1
POBDS/60%NanoG	6.5	−2.6

[a] 600 mV_{SCE} under O_2 condition.
[b] −240 mV_{SCE} under H_2 condition.

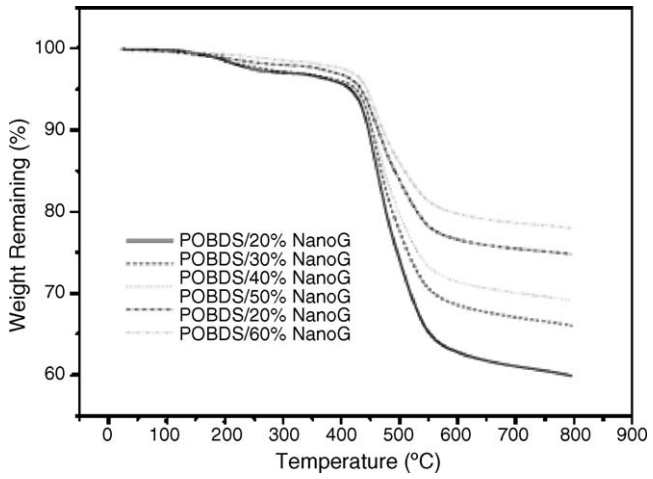

Fig. 15. TGA curves of POBDS/NanoG composites.

The temperature values of 5% weight loss for 20%, 30%, 40%, 50%, 60% NanoG/POBDS composites are 415.62, 425.5, 423.8, 433.7, 443.7, respectively. It could be concluded that POBDS/NanoG composites have a better thermal stability with more NanoG content, due to the excellent thermal stability of NanoG. However, It is clear that all the composites showed a good thermal stability at 80 to 100 °C, which is the temperature range of PEMFC's working environment.

Fig. 16 presents the TGA curves of POBDS/50%NanoG and POBDS/50%EG composites. POBDS/50%EG composite lost 5% of its weight at the temperature of 400.2 °C, which is lower than the counterpart of all POBDS/NanoG composites fabricated in this work. It also could be seen from Fig. 15 that the two kinds of composites have a different degradation behavior. POBDS/50%EG composite underwent more degradation from 200 °C to 400 °C than POBDS/50%NanoG but the latter has a abrupt slope of TGA curve at the range of 400 to 600 °C, indicating that POBDS/50%NanoG composite has a better thermal stability under 400 °C. The NanoG were more effective to prevent POBDS from degradation under the critical temperature of 400 °C. However, POBDS will start degrading massively above 400 °C. Finally, the weight remaining of both kinds was almost

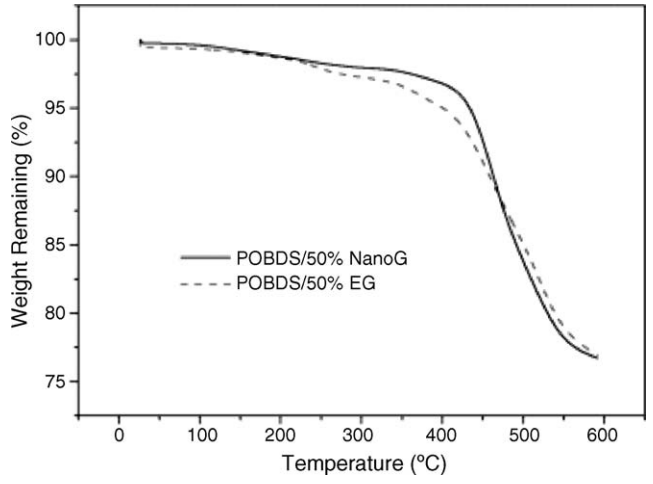

Fig. 16. TGA curves of POBDS/50%NanoG and POBDS/50%EG composites.

the same, because the weight loss was attributed to the degradation of POBDS and the two composites had the same POBDS content.

4. Conclusions

POBDS/graphite nanosheet (NanoG) composites were fabricated using ultrasonic irradiation. Compared to the POBDS/EG nanocomposite previously fabricated, they had better properties: low porosity, low water adsorption, higher flexural strength and higher electrical conductivity. SEM observations revealed that graphite nanosheets were dispersed uniformly in POBDS/NanoG and its surface was smoother than that of POBDS/EG. Also, they had excellent thermal stability and corrosion resistance in a simulated working environment of the polymer electrolyte membrane fuel cell (PEMFC). Therefore, POBDS/NanoG overcome the disadvantages of the POBDS/EG nanocomposite as used in bipolar plates and is a good candidate for the bipolar plates of a PEMFC. In this paper, POBDS/50%NanoG had the best potential for bipolar plates, due to its flexural strength of 32.05 MPa, electrical conductivity of 158.7 S cm^{-1} and its porosity was 8.96×10^{-2}% and it had excellent electrochemical properties.

Acknowledgement

The authors would like to thank the China High-Tech Development 863 Program (Grant No. 2003AA302410), Guangdong Province Sci & Tech Bureau (Key Strategic Project Grant No. 2003C105004, A1100402), and Guangzhou Sci & Tech Bureau (2005U13D2031) for financial support of this work.

References

[1] M.A.J. Cropper, S. Geiger, D.M. Jolie, J. Power Sources 131 (2004) 57–61.
[2] D.S. Scott, Int. J. Hydrogen Energy 29 (2004) 1439–1442.
[3] S. Gottesfeld, T. Zawodzinki, Adv. Electrochem. Sci. Eng. 5 (1997) 195–201.
[4] Y.Z. Meng, Polymer-graphite nanocomposites, in: Polymer Nanocomposites, Woodhead Publishing Limited, Abington, Cambridge, England, CRC press LLC, Boca Raton, 2006, pp. 500–539.
[5] W. Zheng, S.C. Wong, H.J. Sue, Polymer 43 (2002) 6767–6773.
[6] X.M. Chen, J.W. Shen, W.Y. Huang, J. Mater. Sci. Lett. 21 (2002) 213–214.
[7] Y.X. Pan, Z.Z. Yu, Y.Z. Ou, G.H. Hu, J. Polym. Sci., Part B: Polym. Phys. 38 (2000) 1626–1633.
[8] G.H. Chen, D.J. Wu, W.G. Weng, B. He, W.L. Yan, Polym. Int. 50 (2001) 980–985.
[9] G.H. Chen, D.J. Wu, W.G. Weng, B. He, W.L. Yan, J. Appl. Polym. Sci. 82 (2001) 2506–2513.
[10] G.H. Chen, D.J. Wu, W.G. Weng, B. He, C.L. Wu, Carbon 41 (2003) 579–625.
[11] W. Zheng, S.C. Wong, Compos. Sci. Technol. 63 (2003) 225–235.
[12] P. Xiao, M. Xiao, K.C. Gong, Polymer 42 (2001) 4813–4816.
[13] M. Xiao, B. Feng, K.C. Gong, Energy Conver. Manage. 43 (2002) 103–108.
[14] M. Xiao, B. Feng, K.C. Gong, Solar Energy Materi. Solar Cells 69 (2001) 293–296.
[15] L.N. Song, M. Xiao, X.H. Li, Y.Z. Meng, Mater. Chem. Phys. 93 (2005) 122–128.
[16] Y.Z. Meng, S.C. Tjong, A.S. Hay, Polymer 42 (2001) 5215–5224.
[17] Y.Z. Meng, A.S. Hay, J. Appl. Polym. Sci. 74 (1999) 3069–3077.

[18] G.H. Chen, C.L. Wu, W.G. Weng, D.J. Wu, W.L. Yan, Polymer 44 (2003) 1781–1784.
[19] J.M. Lu, X.L. Zhu, J. Zhu, J. Yu, J. Appl. Polym. Sci. 66 (1997) 129–136.
[20] N. Cao, W. Shen, S. Wen, Y. Liu, Chem. Bull. 4 (1996) 37–42.
[21] G.H. Chen, W.G. Weng, D.J. Wu, C.L. Wu, Eur. Polym. J. 39 (2003) 2329–2335.
[22] G.H. Chen, C.L. Wu, W.G. Weng, D.J. Wu, W.L. Yan, Polymer 44 (2003) 1784.
[23] C.E. Borroni-Bird, J. Power Sources 61 (1996) 33–48.